

Corrosion Resistance of Alloy 740 as Superheater Tubing in Coal-Fired Ultra-Supercritical Boilers

Brian A. Baker and Gaylord D. Smith
Special Metals Corporation
3200 Riverside Drive
Huntington, WV 25705-1771

ABSTRACT

The nature of coal ash corrosion and factors affecting its severity are examined. Laboratory results for iron- and nickel-base alloys from a number of sources are compared. Flue gas composition (SO₂ content), coal ash alkali sulfate content, surface temperature and alloy composition are related to corrosion behavior. Results from in situ plant exposures will also be discussed; the role of key alloying elements will be addressed.

Keywords: coal ash corrosion, oxidation, sulfidation, alkali sulfates, laboratory testing, field exposure, alloying elements, ferritic steels, austenitic stainless steels, nickel-containing alloys

INTRODUCTION

The goal of increasing efficiency of future coal-fired power plants necessitates the use of materials having strength and corrosion properties which are greatly improved over those more commonly used ferritic and austenitic steels. Operating conditions for the next generation of ultra-supercritical boiler steam superheaters are expected to have surface temperatures on the order of 700-750°C with 375 bar steam pressure. Alloys selected for use in the form of superheater tubing would thus need to possess high creep rupture strength (100,000 hours rupture life at 100 MPa stress at 750°C). In addition to the strength requirement, the required maximum corrosion loss should be less than 1mm in 100,000 hours. Nickel-base superalloys are being considered in the interest of meeting these stringent demands. Figure 1 shows a compilation of stress rupture data for INCONEL[®] alloy 740 hot-rolled solution-annealed and aged bar and plate, representing data gathered at temperatures from 700°C to 800°C. Using the fitted power law averaged curve shown, a stress of 145 MPa is predicted to produce rupture in 100,000 hours at 750°C.

Reviews on the mechanisms governing coal ash corrosion have been done.^{1,2} Plant and laboratory studies have shown that the most relevant mechanism is related to the formation of molten alkali trisulfates, and the corrosion rate can be strongly related to operating temperature (see Figures 2 to 4).³⁻⁶ This mechanism falls under the definition of Type II hot corrosion, whereby fluxing of scales results from contact with molten, alkali-containing sulfates.⁷⁻⁸ The characteristic bell-shaped curve when

[®]INCONEL is a registered trademark of the Special Metals family of companies.

plotting wastage rate versus temperature results from phase changes occurring for sodium-potassium-iron trisulfates. Below about 600°C, corrosion activity is thought to be low because trisulfate exists in solid form. Above about 750°C, corrosion rates again drop as trisulfates vaporize. Between 600°C and 750°C, where trisulfates exist in a molten state, corrosion rates are thought to be maximized.⁹ Incorporation of additional metallic elements other than iron into the sulfate mixture may serve to 'shift' the bell curve, resulting in variation in the temperature at which the maximum corrosion rate is observed.

This work focused upon laboratory corrosion results obtained for nickel-base superalloys, in addition to nickel-chromium alloys. The kinetics of observed corrosion attack were examined and corrosion mechanisms were verified via microstructural examination.

EXPERIMENTAL PROCEDURE

The nickel-base alloys 740 (and several experimental variants thereof, including alloys A-1 and A-2), 617, 690, 671, 693, 90, 105, a variant of alloy 91 (termed alloy B) and 803 were studied. Compositions for these alloys, and those from discussed referenced studies, are shown in Table 1. Experiments were carried out at 700°C and 775°C in SO₂-bearing gaseous environments with alkali sulfate-containing coatings applied to the sample surface, in order to simulate fireside coal ash deposition.

The ash mixtures consisted of 2.5-5% Na₂SO₄-2.5-5% K₂SO₄-90-95% (Fe₂O₃-Al₂O₃-SiO₂ in 1:1:1 ratio by weight). The ash mixture was prepared by grinding with mortar and pestle. The synthetic flue gas was mixed using electronic flow meters from component gases (including a pre-mixed cylinder of N₂-1.8% SO₂) and consisted of N₂ - 15% CO₂ - 3.5% O₂ - 0.25% SO₂ (or N₂ - 15% CO₂ - 4% O₂ - 1% SO₂). Test samples consisted of 7.6 mm diameter X 19 mm long cylindrical pins machined to a 32 microinch finish. Prior to testing, the synthetic coating was applied to the samples surfaces by first diluting with acetone and then using a bristle brush. The approximate mass gain resulting from application of the coating was 40 mg/cm². Samples were allowed to dry completely before testing. The coated samples were placed in a cordierite ceramic boat and exposed in a sealed horizontal, electrically heated muffle furnace having a 100 mm OD mullite tube. Samples were placed into the heated section of the furnace after sufficient purging and introduction of the test gas, using a sealed pushrod mechanism. Samples were cycled at approximately 500 h, 1000 h, 2000 h and 4000 h. Exfoliated surface products were removed and the coating was re-applied after each of the given time intervals.

Metal loss and average depth of attack were assessed from sample cross sections. Average values for metal loss and depth of attack were determined from a total of six measurements made around the circumference of each pin. In the case of the depth of attack measurement, the maximum depth of intrusion was determined for each of the six fields examined at approximately 60 degree intervals around the circumference of the pin. Structural analyses were carried out using optical microscopy and SEM/EDS.

RESULTS AND DISCUSSION

Figure 5 shows depth of attack measurements for several nickel-base alloys tested at 700°C and 775°C in a gas mixture comprised of N₂ - 15% CO₂ - 4% O₂ - 1% SO₂ with the samples having a salt consisting of 2.5% Na₂SO₄-2.5% K₂SO₄-95% (Fe₂O₃-Al₂O₃-SiO₂ in 1:1:1 ratio by weight) applied to the surface. Except for the alloy 188, all materials tested showed decreased corrosion activity at the higher testing temperature. The unique behavior of alloy 188 may be due to its higher Co content causing a shift in

the temperature at which the peak corrosion rate is observed, relative to the other alloys tested. Figure 5 shows depth of attack results versus chromium level for each alloy tested, in comparison with data reported by Blough and Stanko¹⁰ and Castello, et al.¹¹ Alloy 740 (740-3, chemistry shown in Table 1, was part of the study done by Castello, et al.). The results are plotted in semi-logarithmic fashion in order to more readily compare the results. The results agree reasonably well. The inverse relationship of chromium content to the observed corrosion rate is reinforced. Beyond 25-30% chromium, little change is observed from increasing the chromium level further.

Figure 7 shows depth of attack measurements for alloys tested at 700°C in a gas mixture comprised of N₂ - 15% CO₂ - 3.5% O₂ - 0.25% SO₂ with the samples having a salt consisting of 5% Na₂SO₄-5% K₂SO₄-95% (Fe₂O₃-Al₂O₃-SiO₂ in 1:1:1 ratio by weight) applied to the surface. Alloys 617, A1 and A2 (alloy 740 with 6% Mo) suffered significant thickness loss, exhibiting linear kinetics. These results could indicate that molybdenum at 6-9% is undesirable for coal ash corrosion resistance, under the examined conditions. Perhaps incorporation of molybdenum into the trisulfate ash forming at the material surface leads to an increased corrosion rate by affecting the solubility of protective chromium oxides, as observed in Mo-containing alloys which undergo high temperature Type I hot corrosion at about 825-950°C.^{7,12} Results for alloy 263, another 6% molybdenum material, were similar to those obtained for alloy 617 in the data shown in Figure 5 as well. Kinetics of alloys 740, 693, 690 and 671 were more parabolic in nature. Figure 8 shows these results plotted against those reported by Blough and Stanko¹⁰ and Castello, et al.¹¹ under similar conditions. Reasonable agreement was obtained. Again, once the chromium level exceeds 25-30%, corrosion activity stabilizes.

Alloy 740 has been exposed in a test loop within a subcritical coal fired boiler burning 3-3.5% sulfur Ohio coal and evaluated after 21,200 hours of operation (11,288 hours of exposure at full temperature, due to outages and dispatch).¹³ Figure 8 shows the locations of specimens within the test loop. Samples were in the form of 2.5 inch diameter by 0.400" wall by six inches in length and were joined by GTAW with filler metal 625. Samples are letter coded in Figure 9, in order from inlet to outlet (coldest to hottest temperature). Table 2 shows metal loss rate and average surface metal temperature for each sample tested. Figure 9 shows metal wastage plotted as a function of average metal surface temperature. The best-performing materials in the test were high-chromium nickel-base materials and included alloy 671/800HT clad, filler metal 52 weld overlay, filler metal 72 weld overlay and alloy 740. Figure 10 shows metal wastage plotted as a function of average metal surface temperature.

CONCLUSIONS

Based upon the results of this and similar laboratory studies of the resistance of various materials to simulated alkali sulfate coal ash conditions, alloy 740 holds encouraging promise for service in ultra-supercritical boiler steam superheaters. The combination of strength (easily meeting the requirement of 100,000 hour rupture life at 750°C/100 MPa), corrosion resistance and fabricability to a variety of product forms make alloy 740 unique in its capabilities.

Recent results for alloy 740 exposed in actual coal-fired boiler service, at metal surface temperatures ranging from 569°C to 627°C and under severe conditions, also indicate the viability of this material for such service.

REFERENCES

1. M. Hoffman, IAM-JRC, European Commission, for INCO No. 13382, 1997.

2. I. M. Rehn, Foster Wheeler Development Corporation, for EPRI No. 1403-11, 1987.
3. M. Tamura, N. Yamanouchi, M Tanimura, S. Murase, "Promising Alloys for the Heat Exchangers of Advanced Coal Fired Boilers," Proceedings : Exposition and Symposium on Industrial Heat Exchanger Technology (Materials Park, Ohio: ASM International 1985), p. 273.
4. H. Teranishi, *et al*, presented at the International Conference on High Temperature Alloys, Preprint Paper No. 21, Petten, The Netherlands, Oct 15-17, 1985
5. Ohtomo, *et al*, High Temperature Corrosion Characteristics of Superheater Tubes, Ishikawajima Harima Industries, *Engg. Rev.*, Vol. 16 (No. 4), Oct. 1983.
6. J. L. Blough , *et al*, Superheater Corrosion in Ultra-Supercritical Power Plants, CORROSION/2000, Paper No. 0250, NACE International, Houston, TX, 2000.
7. R. A. Rapp and Y. S. Zhang, Hot Corrosion of Materials: Fundamental Studies, JOM, Vol. 46. No. 12, 1994, p. 47.
8. G. R. Holcomb, Hot Corrosion in a Temperature Gradient, Materials and Corrosion ,51, 2000, p. 564.
9. R. Viswanathan and W. T. Bakker, Proceedings: 2000 International Joint Power Generation Conference, Miami Beach, Florida, July 23-26, 2000.
10. J. L. Blough and G. J. Stanko, Fireside Corrosion Testing of Candidate Superheater Tube Alloys, Coatings and Claddings - Phase II, CORROSION/97, Paper No. 140, NACE International, Houston ,TX, 1997.
11. Castello, P., Guttman, V., Farr, N.*, Smith, G., Laboratory Simulated Fuel-Ash Corrosion of Superheater Tubes in Coal-Fired Ultra Supercritical-Boilers, Proceedings of the EUROMAT Conference, 27-30 September 1999, München (D), Wiley-VCH Verlag - ORA/PRO 60750.
12. J. A. Goebel, et al., Mechanisms for Hot Corrosion of Nickel-Base Alloys, Metallurgical Transactions, Vol. 4, 1973, pp. 261-278.
13. D. K. McDonald, Coal Ash Corrosion Resistant Materials Testing Program Evaluation of the First Section Removed in November 2001, The Babcock and Wilcox Company, submitted to DOE (DE-FC26-99FT40525) and OCDO (CDO/D-98-2).

Table 1. Chemical Composition (Weight %) for the Alloys of This Study

Alloy	C	Mn	Fe	Si	Ni	Cr	Al	Ti	Co	Mo	Nb+Ta	W
740-1 [†]	0.074	0.30	1.1	0.51	47.3	25.3	0.84	1.93	19.91	0.59	2.01	-
740-2 [†]	0.074	0.28	1.1	0.52	47.7	25.0	0.82	1.95	19.84	0.53	2.05	-
740-3 [†]	0.060	0.30	0.7	0.47	48.5	25.0	0.87	1.69	19.80	0.58	2.01	-
740-4 [†]	0.032	0.28	1.0	0.49	51.2	23.0	0.72	1.63	19.27	0.51	1.87	-
740-5*	0.070	0.30	2.1	0.50	49.0	23.5	0.70	2.00	19.50	0.40	2.00	-
A-1 [†]	0.109	0.29	0.6	0.33	43.9	24.1	0.63	2.02	19.79	5.85	2.02	-
A-2 [†]	0.037	0.30	0.6	0.52	44.9	23.5	0.57	1.63	19.96	5.86	2.00	-
693 [§]	0.020	0.20	4.0	0.10	61.0	29.0	3.10	0.40	-	-	0.60	-
690 [§]	0.030	0.20	10.0	0.05	59.0	29.0	0.25	0.30	-	-	-	-
FM52	0.030	0.20	9.0	0.20	59.0	29.0	0.60	0.60	-	-	-	-
FM72	0.020	-	0.2	0.10	56.0	43.0	0.15	0.50	-	-	-	-
617 [§]	0.085	0.10	1.5	0.10	54.0	22.0	1.10	0.30	11.50	9.60	0.10	-
105 [§]	0.10 Max.	1.0 Max.	1.0 Max.	1.0 Max.	53.0	15.0	4.70	1.20	20.00	5.00	-	-
90 [§]	0.13 Max.	1.0 Max.	1.5 Max.	1.0 Max.	53.0	20.0	1.50	2.50	18.00			-
671 [§]	0.030	-	-	-	52.5	46.5	0.30	0.40	0.10	-	-	-
671 Cladding [§]	0.050	-	0.2	0.20	51.0	48.0	-	0.40	-	-	-	-
263 [§]	0.050	0.35	0.5	0.10	51.0	20.0	0.50	2.10	19.50	5.80	-	-
B [†]	0.090	0.20	0.5	0.80	51.0	28.0	0.20	1.50	20.00	0.10	0.10	-
HR120 [§]	0.050	0.70	Bal.	0.60	37.0	25.0	0.10	-	-	2.5 Max.		2.5 Max.
803 [§]	0.070	0.90	Bal.	0.70	34.5	25.5	0.50	0.50	-	0.30	-	-
800 Mod.*	0.100	1.93	Bal.	0.25	31.0	19.9	-	0.10	-	1.50	0.25	-
NF 709 [§]	0.070	1.00	Bal.	0.60	25.0	20.0	-	0.60	-	1.50	0.20	-
188 [§]	0.095	0.80	1.5	0.30	23.5	22.0	0.20	-	37.00	-	-	14.00
310 Ta*	0.060	1.70	Bal.	0.25	21.3	23.8	-	-	-	-	-	-
310 HCBN [§]	0.060	1.20	Bal.	0.40	20.0	25.0	-	-	-	-	1.50	-
SAVE 25 [§]	0.100	1.00	52.0	0.40	18.0	20.0	-	-	-	-	0.45	1.50
347HFG [§]	0.080	2.00	Bal.	1.00	11.0	18.0	-	-	-	-	10XC Min.	
Fe ₃ Al [†]	0.008	-	Bal.	-	-	1.6	15.79	-	-	-	-	-

† - Actual Composition

§ - Nominal Composition

* - Average Composition (Multiple Heats)

Table 2. Metal Loss Measurements Reported by McDonald for Samples Exposed in a Coal Fired Boiler Test Loop¹³

Material	Tube Sample Label	Metal Loss Rate (mils/yr)	Metal Loss Rate (mm/yr)	Average Surface Metal Temperature, °F	Average Surface Metal Temperature, °C
Save 25	AA	259	6.6	1170	632
Save 25	T	224	5.7	1146	619
Save 25	K	209	5.3	1084	584
Save 25	B	67	1.7	1047	564
800 Mod	AB	169	4.3	1174	634
800 Mod	U	178	4.5	1150	621
800 Mod	L	154	3.9	1092	589
347 HFG	H	176	4.5	1075	579
347 HFG	Y	174	4.4	1164	629
347 HFG	Q	83	2.1	1137	614
NF 709	A	170	4.3	1167	631
NF 709	I	145	3.7	1077	581
NF 709	S	136	3.5	1142	617
Fe3Al	R	145	3.7	1139	615
310 Ta	V	136	3.5	1154	623
310 Ta	AC	123	3.1	1178	637
310 Ta	M	120	3.0	1092	589
310 HCbN	W	133	3.4	1157	625
310 HCbN	J	129	3.3	1081	583
310 HCbN	AD	108	2.7	1180	638
310 HCbN	N	98	2.5	1095	591
HR120	G	109	2.8	1077	581
HR120	AE	102	2.6	1184	640
HR120	O	61	1.5	1100	593
740-5	X	53	1.3	1160	627
740-5	C	31	0.8	1056	569
FM52 WO	D	77	2.0	1062	572
FM52 WO	AH	44	1.1	1198	648
FM72 WO	E	21	0.5	1068	576
FM72 WO	AG	10	0.3	1198	648
671 Clad	F	13	0.3	1075	579
671 Clad	P	2	0.1	1110	599
671 Clad	AF	4	0.1	1193	645

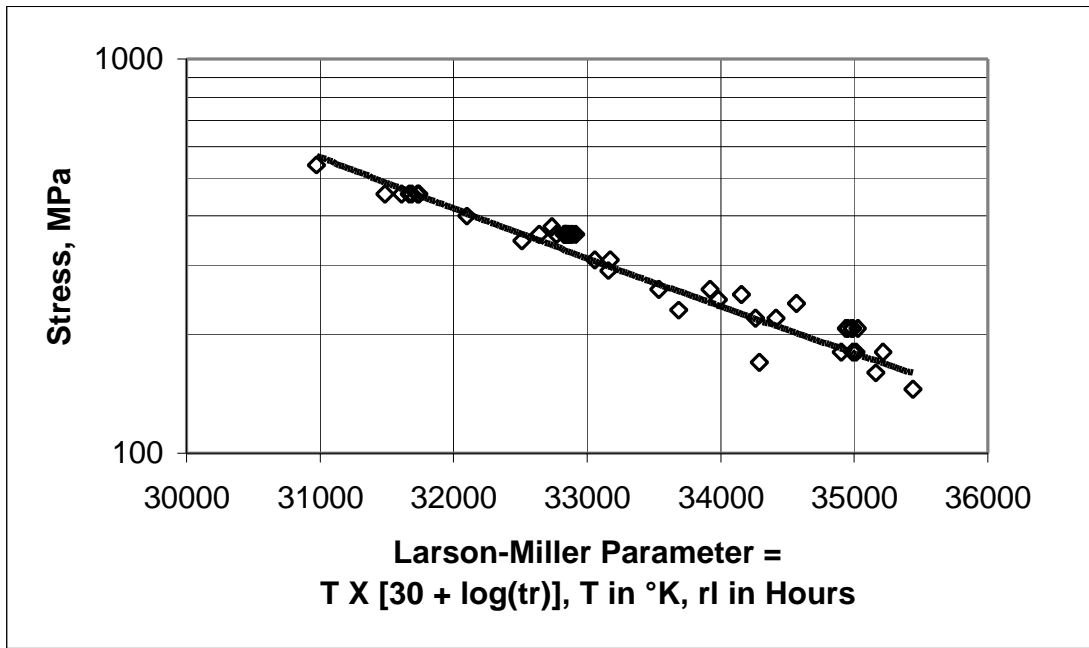


Figure 1. Stress rupture data compilation for hot-rolled solution-annealed and aged alloy 740 bar and plate, showing power law fit.

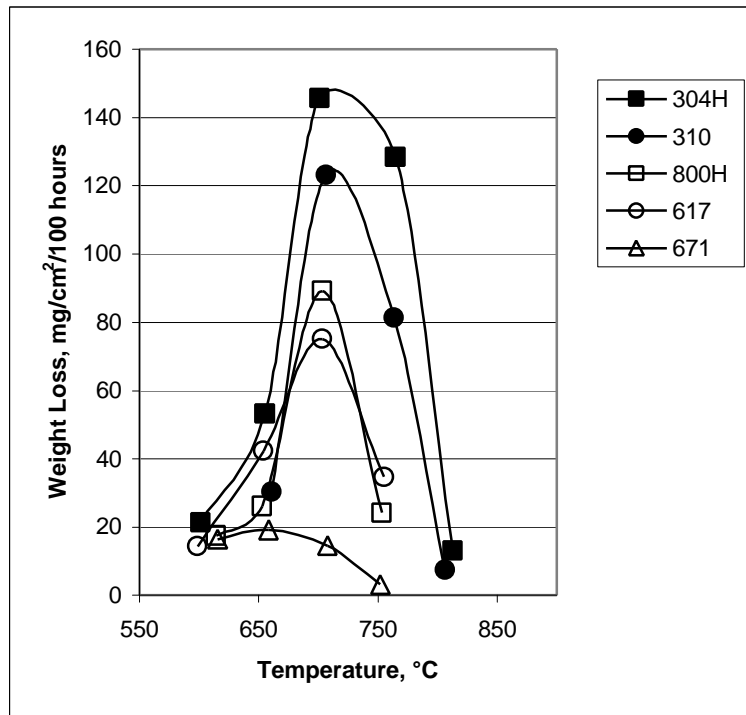


Figure 2. Dependence of corrosion behavior in synthetic coal ash/flue gas corrosion upon temperature.³ Gas composition = 1%SO₂-5% O₂-15%CO₂-Bal. N₂. Synthetic ash = 34%Na₂SO₄41%K₂SO₄-25%Fe₂O₃.

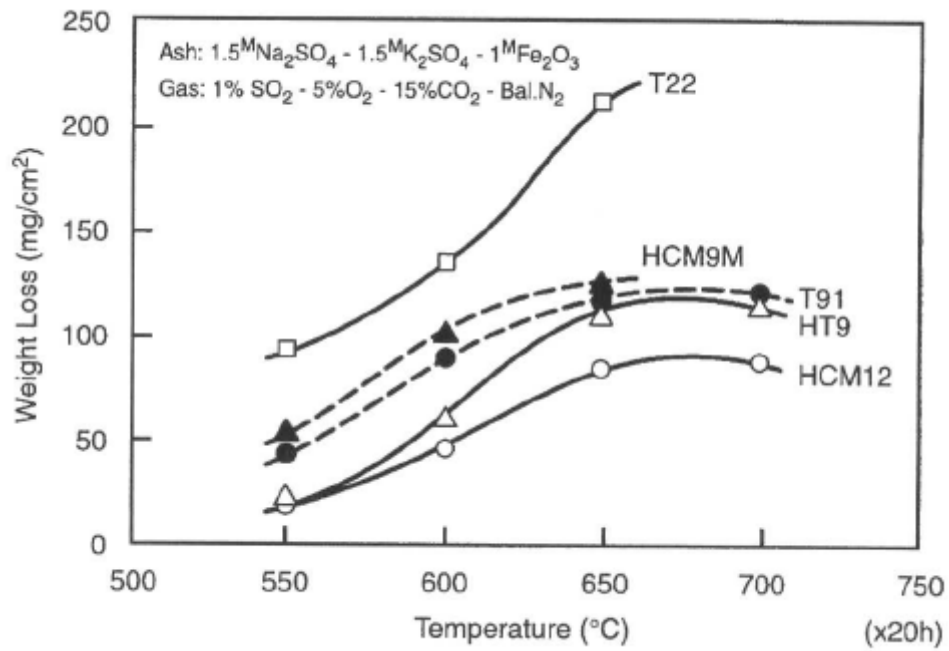


Figure 3. Relationship between hot corrosion weight loss and temperature for ferritic steels.⁴

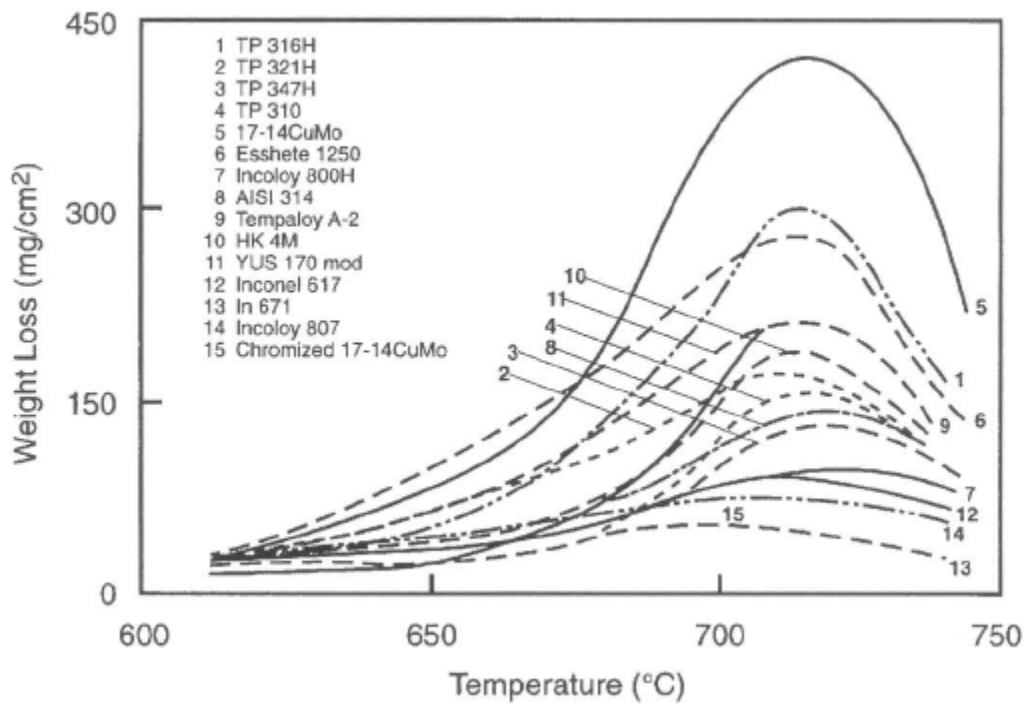


Figure 4. Comparison of fire-side corrosion resistance of various alloys as a function of temperature.⁵

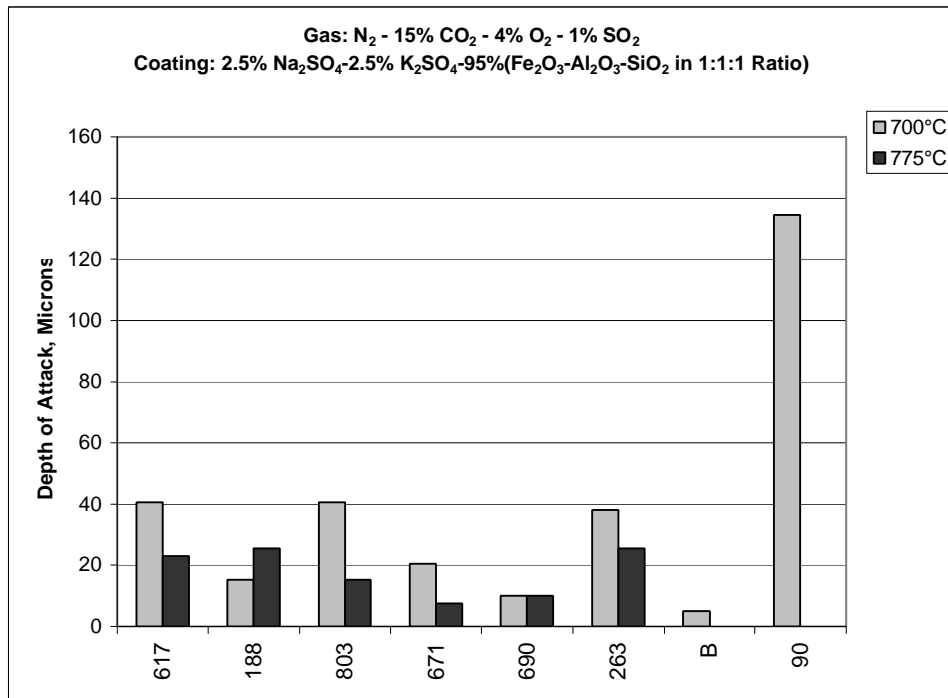


Figure 5. Depth of attack after 1008 hours of exposure in a simulated coal-fired boiler environment, at 700°C and 775°C. Samples were coated only once at the beginning of the test.

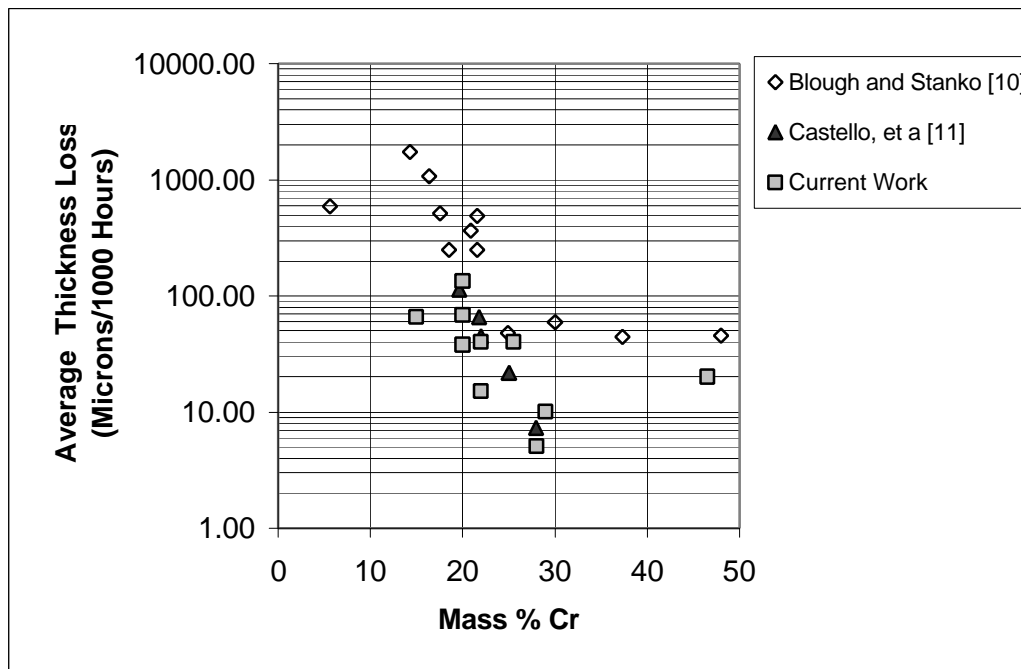


Figure 6. Cross section loss (depth of attack) for high temperature alloys exposed at 700°C in laboratory flue gases (1% SO₂) with alkali sulfate-oxide coatings applied to the sample surface, as a function of chromium content.

[10]: N₂-14%CO₂-10%H₂O-3.6%O₂-1%SO₂, 10% alkali sulfates

[11]: N₂-15%CO₂-3.5%O₂-1%SO₂, 10% alkali sulfates

Current Work: N₂-15%CO₂-4%O₂-1%SO₂, 5% alkali sulfates

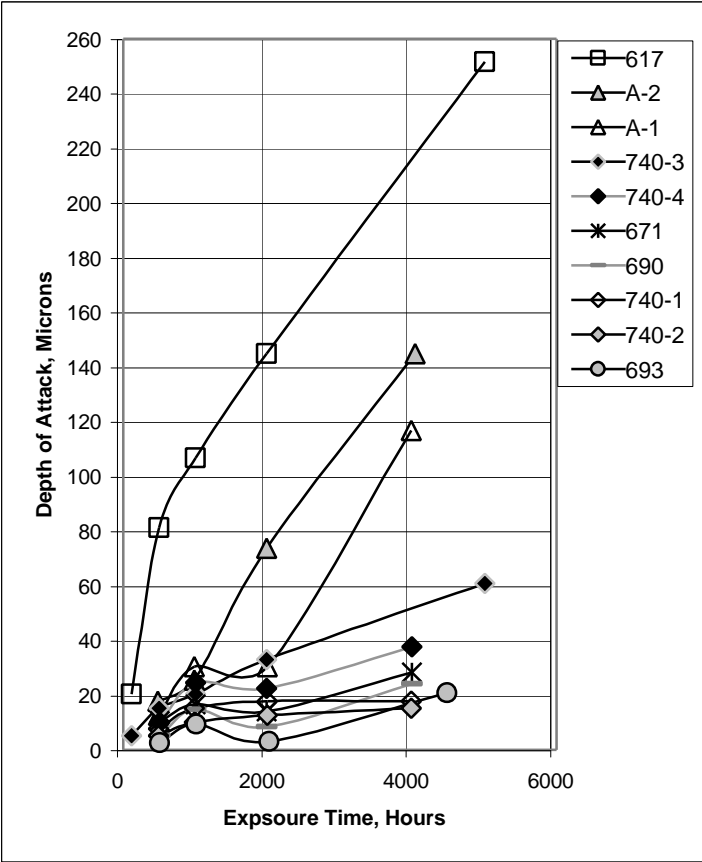


Figure 7. Depth of attack after exposure at 700°C in N₂ - 15% CO₂ - 3.5% O₂ - 0.25% SO₂ with samples having a salt consisting of 5% Na₂SO₄-5% K₂SO₄-95% (Fe₂O₃-Al₂O₃-SiO₂ in 1:1:1 ratio by weight) applied to the surface (re-coated at the intervals shown).

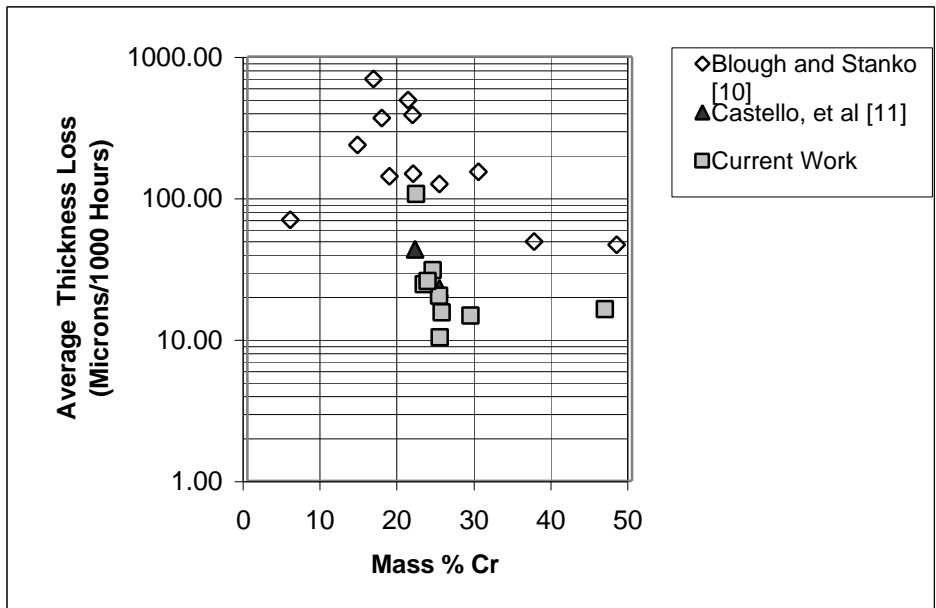


Figure 8. Cross section loss (depth of attack) for high temperature alloys exposed at 700°C in laboratory flue gases (0.25% SO₂) with alkali sulfate-oxide coatings applied to the sample surface, as a function of chromium content.

[10]: N₂-14%CO₂-10%H₂O-3.6%O₂-0.25%SO₂, , 10% alkali sulfates

[11]: N₂-15%CO₂-3.5%O₂ -0.25%SO₂, 10% alkali sulfates

Current Work: N₂-15%CO₂-3.5%O₂ -0.25%SO₂, 10% alkali sulfates

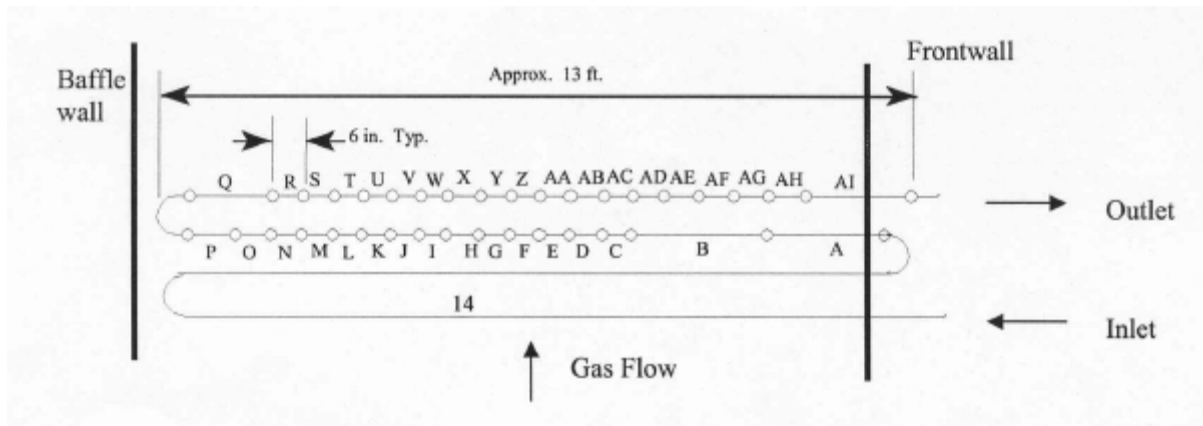


Figure 9. Numbering of specimens within test loop exposed in a subcritical coal fired boiler firing 3-3.5% sulfur Ohio coal.¹²

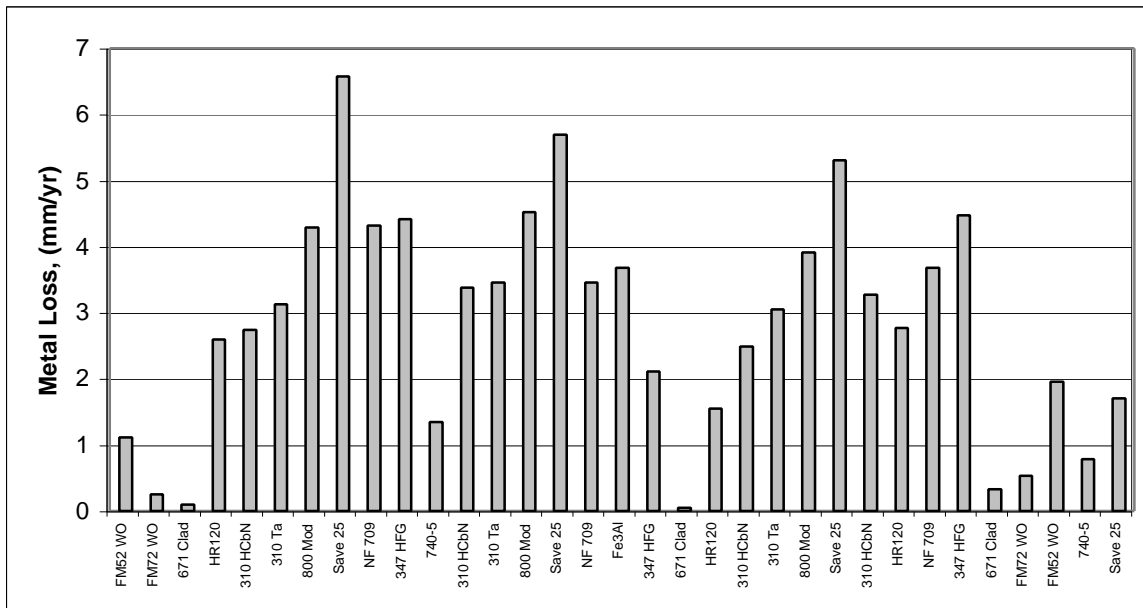


Figure 10. Metal loss as a function of position in test loop exposed in coal fired boiler firing 3-3.5% S Ohio coal. Results reported by McDonald.¹³